Mineralogical Magazine (2023), 1–10
doi:10.1180/mgm.2023.29

CAMBRIDGE UNIVERSITY PRESS

Article

Bystrite, $Na_7Ca(Al_6Si_6O_{24})S_5^{2-}Cl^-$: formula redefinition and relationships with other four-layer cancrinite-group minerals

Nikita V. Chukanov[1,2], Anatoly N. Sapozhnikov[3], Ekaterina V. Kaneva[3], Dmitry A. Varlamov[4] and Marina F. Vigasina[2]

[1]Federal Research Center of Problems of Chemical Physics and Medicinal Chemistry, Russian Academy of Sciences, Chernogolovka, Moscow region, 142432 Russia; [2]Faculty of Geology, Moscow State University, Vorobievy Gory, Moscow, 119991 Russia; [3]Vinogradov Institute of Geochemistry, Siberian Branch of Russian Academy of Sciences, 1a Favorskii St., Irkutsk, 664033, Russia; and [4]Korzhinskii Institute of Experimental Mineralogy, Russian Academy of Sciences, 142432 Chernogolovka, Russia

Abstract

Bystrite is redefined as a four-layer cancrinite-group mineral with the four-layer Losod-type framework and the end-member formula $Na_7Ca(Al_6Si_6O_{24})S_5^{2-}Cl^-$. The mineral is known only at the Malo–Bystrinskoe gem lazurite deposit, Baikal Lake area, Siberia, Russia. The associated minerals are calcite, lazurite, sodalite, fluorapatite, phlogopite, diopside, dolomite and plagioclase. Bystrite is brittle, with the Mohs hardness of 5 and distinct cleavage on $\{10\bar{1}0\}$. The yellow colour of bystrite is due to the presence of S_5^{2-} anions occurring in Losod (LOS) cages of the aluminosilicate framework with the *ABAC* stacking sequence. Measured and calculated density is, respectively, 2.43(1) and 2.412 g cm^{-3} for the holotype and 2.42(1) and 2.428 g cm^{-3} for the cotype sample. Bystrite is uniaxial (+), $\varepsilon = 1.660(2)$ and $\omega = 1.584(2)$. The mineral was characterised by infrared and Raman spectra. The empirical formulae of the holotype and cotype samples are $Na_{6.97}K_{0.04}Ca_{0.98}(Si_{6.03}Al_{5.97}O_{24})(S_5^{2-})_{0.93}[(SO_4^{2-})_{0.15}Cl_{0.83}]$ and $Na_{6.75}K_{0.04}Ca_{1.11}(Si_{6.09}Al_{5.91}O_{24})(S_5^{2-})_{1.04}[(HS^-)_{0.17}Cl_{0.85}]$, respectively. Bystrite is trigonal, space group *P*31*c*. The unit-cell parameters are: $a = 12.8527(6)$ Å, $c = 10.6907(5)$ Å, $V = 1529.4(1)$ Å^3 and $Z = 2$. The strongest lines of the powder X-ray diffraction pattern [*d*, Å (*I*, %) (*hkl*)] are: 4.821 (32) (102), 3.915 (38) (211), 3.712 (100) (300), 3.307 (50) (212), 2.782 (18) (400), 2.692 (22) (401), 2.673 (30) (004) and 2.468 (23) (402). Isomorphism and genesis of bystrite-type minerals is discussed. Bystrite and its K,HS-analogue sulfhydrylbystrite, $Na_5K_2Ca(Al_6Si_6O_{24})S_5^{2-}(HS)^-$, are indicators of highly reducing conditions.

Keywords: bystrite, cancrinite group, formula redefinition, IR spectroscopy, Raman spectroscopy, Malo–Bystrinskoe deposit

(Received 9 January 2023; accepted 10 April 2023; Accepted Manuscript published online: 19 April 2023; Associate Editor: Owen Missen)

Introduction

Cancrinite-group minerals are microporous trigonal or hexagonal aluminosilicates. Their frameworks consist of layers composed by six-membered rings of Si- and Al-centred tetrahedra perpendicular to the *c* axis. The rings around the [0 0 *z*], [⅔ ⅓ *z*] and [⅓ ⅔ *z*] axes, as well as the layers formed by these rings are denoted by the letters *A*, *B* and *C*, respectively (Rinaldi and Wenk, 1979; Ballirano *et al.*, 1996).

Bystrite was first described as a trigonal (space group *P*31*c*) cancrinite-related mineral with the unit-cell parameters $a = 12.855$ Å and $c = 10.700$ Å, and the simplified formula $Ca(Na,K)_7(Al_6Si_6O_{24})(S_3^{2-})_{1.5}\cdot H_2O$ (Sapozhnikov *et al.*, 1991; Pobedimskaya *et al.*, 1991). Initially, two bystrite varieties have been distinguished: (1) K-rich and Cl-deficient and (2) Cl-rich and K-poor varieties. The former mineral has been approved as the separate mineral species sulfhydrylbystrite with the formula $Na_5K_2Ca(Al_6Si_6O_{24})S_5^{2-}(HS)^-$ derived on the basis of chemical data and X-ray structural analyses (Sapozhnikov *et al.*, 2017). The crystal structure of sulfhydrylbystrite is based on a four-layer Losod-type framework (the *ABAC* stacking sequence: see the review by Chukanov *et al.*, 2021) hosting small cancrinite (CAN) cages and large Losod (LOS) cages.

According to the International Union of Pure and Applied Chemistry (IUPAC) nomenclature (McCusker *et al.*, 2001), the CAN cage $[4^66^5]$ is limited by six four-membered and five six-membered rings and the LOS cage $[4^66^{11}]$ is limited by six four-membered and eleven six-membered rings. The columns of CAN cages run along the [0 0 *z*] axis. The columns around the [⅓ ⅔ *z*] and [⅔ ⅓ *z*] axes consist of LOS cages.

In sulfhydrylbystrite, LOS cages contain Na^+- and K^+-dominant sites, S_5^{2-} is the dominant anion in the LOS cage and $(HS)^-$ ions dominate over Cl^- in columns of cancrinite cages. These ions are considered as the species-defining components of sulfhydrylbystrite. It is noteworthy that the S_5^{2-} anion is thermodynamically favoured among S_n^{2-} anions for $n = 2$ to 8: the order of decreasing stability in aqueous solution is $S_5^{2-} >> S_6^{2-} > S_4^{2-} >> S_7^{2-} > S_3^{2-} >> S_8^{2-} > S_2^{2-}$ (Steudel and Chivers, 2019).

The crystal structure of the presumed Cl-rich and K-deficient bystrite variety was investigated by Kaneva *et al.* (2017). It was shown that this mineral is isostructural with sulfhydrylbystrite

Corresponding author: Nikita V. Chukanov; Email: chukanov@icp.ac.ru
Cite this article: Chukanov N.V., Sapozhnikov A.N., Kaneva E.V., Varlamov D.A. and Vigasina M.F. (2023) Bystrite, $Na_7Ca(Al_6Si_6O_{24})S_5^{2-}Cl^-$: formula redefinition and relationships with other four-layer cancrinite-group minerals. *Mineralogical Magazine* 1–10. https://doi.org/10.1180/mgm.2023.29

and is its analogue with Cl^- rather than $(HS)^-$ in cancrinite cages, and that is has Na^+ at the site occupied predominantly by K^+ in sulfhydrylbystrite. It has been suggested (Sapozhnikov *et al.*, 2017) that the presumed Cl-rich and K-deficient bystrite variety should be considered as bystrite *s.s.* However, this suggestion has not been discussed in the Commission on New Minerals, Nomenclature and Classification of the International Mineralogical Association (IMA–CNMNC) and the status of bystrite as a mineral species has remained uncertain.

On the basis of data from wet chemical analyses, 96% of total sulfur in bystrite occurs in the sulfide form (Sapozhnikov *et al.*, 1991), however the X-ray structural analysis shows that all sulfur belongs to the S_5^{2-} anion. Minor sulfate sulfur could be partly formed as a result of partial sulfur oxidation during the analysis.

A revised formula of bystrite, $Na_7Ca(Al_6Si_6O_{24})S_5^{2-}Cl^-$, has been approved by the IMA–CNMNC (Nomenclature Voting proposal 22-H, Miyawaki *et al.*, 2023). A four-layer aluminosilicate framework with the *ABAC* stacking sequence, the predominance of S_5^{2-} and Cl^- extra-framework anions in the LOS cages and in the column of CAN cages, respectively, Ca^{2+} cations at the centres of the bases of LOS cages and the absence of K-dominant sites are the species-defining features distinguishing bystrite from other cancrinite-group minerals.

The holotype specimen of bystrite (Sample 1 in this paper) is deposited in the Fersman Mineralogical Museum (Moscow) with the catalogue number 92390. The cotype specimen of bystrite (Sample 2 in this paper) is deposited in the collection of the Sidorov Mineralogical Museum (INRTU), Irkutsk, Russia, registration number MMU/MF 28069.

In this paper, we provide data on bystrite which is a chloride and K-poor analogue of the K- and $(HS)^-$-dominant mineral sulfhydrylbystrite, $Na_5K_2Ca(Al_6Si_6O_{24})S_5^{2-}(HS)^-$ that are required to define this mineral as an individual species, as well as data on isomorphism of four-layer cancrinite-group minerals with the *ABAC* stacking sequence of layers of tetrahedra.

Samples

Data on four samples are presented. Samples 1 and 2 are bystrite. Both samples originate from the Malo–Bystrinskoe gem lazurite deposit, Baikal Lake area, Siberia, Russia. They form yellow anhedral equant grains up to 1 mm across in partly recrystallised lazurite calciphyre (Figs 1a and 2a). The associated minerals are calcite, lazurite, sodalite, fluorapatite, phlogopite, diopside, dolomite and plagioclase $Pl_{34–43}$ (Fig. 1a). Bystrite grains are embedded in calcite granular aggregate. Lazurite and bystrite show no reaction relations. Sodalite forms inclusions in bystrite and lazurite, and dolomite occurs as inclusions in calcite. Locally, bystrite occurs as a component of fine-grained polymineral aggregates in which grains of earlier minerals are partly substituted by phlogopite and plagioclase (Fig. 1b). Bystrite-bearing assemblages have a metasomatic origin (Sapozhnikov *et al.*, 1991).

Sample 1 represents fragments of the bystrite holotype (Sapozhnikov *et al.*, 1991). The holotype specimen of bystrite is deposited in the Fersman Mineralogical Museum (Moscow) with the catalogue number 92390. New data on the chemical composition, infrared and Raman spectra and density (this work), powder and single-crystal X-ray diffraction, crystal structure (Kaneva *et al.*, 2017), as well as optical data (Sapozhnikov *et al.*, 1991) were obtained for this sample. Additionally, for bystrite Sample 2, data on the chemical composition, infrared and Raman spectra, powder X-ray diffraction pattern and density are obtained. Sample 2 is considered as a cotype of bystrite.

Sample 3 is sulfhydrylbystrite previously described by Kaneva *et al.* (2017). Its empirical formula is $H_xNa_{4.37}K_{2.22}Ca_{1.17}(Si_{6.12}Al_{5.87}Fe_{0.01}O_{24})S_{5.86}Cl_{0.09}$, where S is total sulfur (Chukanov *et al.*, 2022d). Sample 3 forms red–orange anhedral grains up to 0.4 mm across in a metasomatic rock mainly composed of calcite, diopside, nepheline, lazurite, afghanite, phlogopite and plagioclase, with Ca- and Ba-bearing stronalsite, $Na_2(Sr,Ca,Ba)(Si_4Al_4O_{16})\cdot nH_2O$, occurring in the rock in different proportions (Figs 2b and 3). Sample 3 is a fragment of the material, another part of which is deposited as the holotype specimen of sulfhydrylbystrite at the Mineralogical Museum of Saint-Petersburg State University (catalogue no. 1/19636).

Sample 4 is a K-rich analogue of bystrite. It occurs in a boudin 12 cm × 8 cm × 6 cm (Fig. 4), found in the year 2000 at the dump of the Malo–Bystrinskoe deposit. The mineral forms yellow grains up to 40 μm × 80 μm (Fig. 5) in an intermediate zone between the inner zone enriched in lazurite and a zone composed of diopside

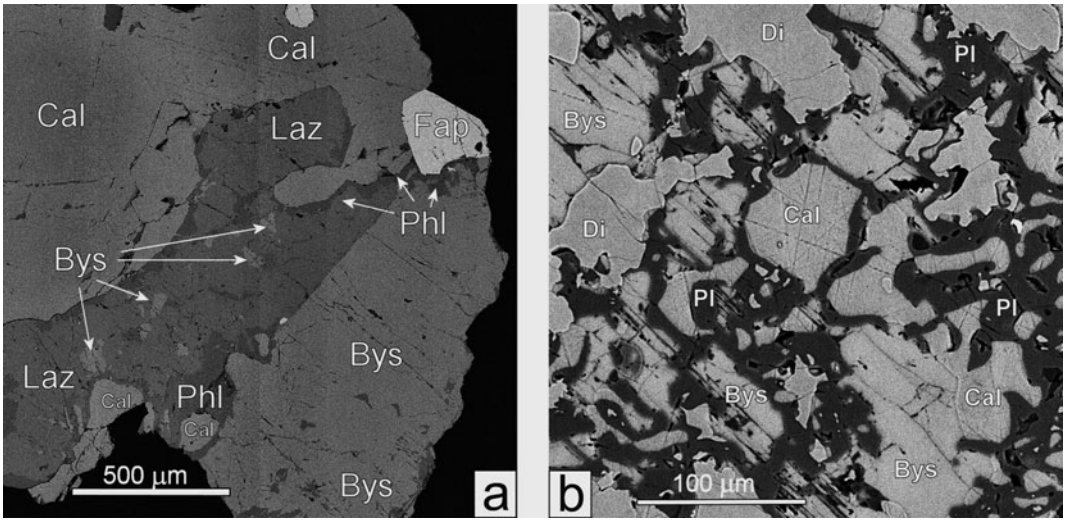

Figure 1. Bystrite (Bys) in association with lazurite (Laz), calcite (Cal), fluorapatite (Fap), phlogopite (Phl), plagioclase (Pl) and diopside (Di). Sample 2. SEM backscattered electron (BSE) images of polished sections; labels from Warr (2021).

https://doi.org/10.1180/mgm.2023.29 Published online by Cambridge University Press

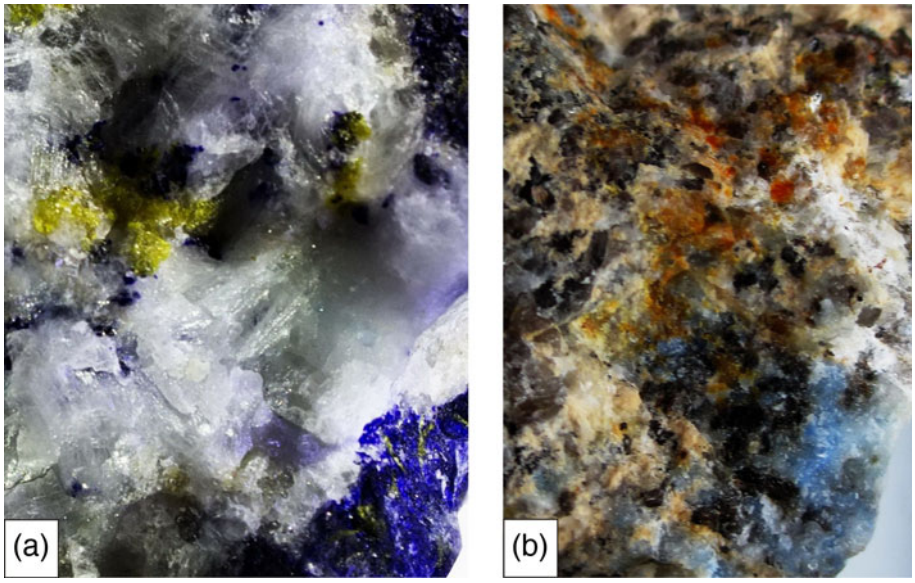

Figure 2. Grains of (a) bystrite (yellow, Sample 1) in association with lazurite (deep blue) and calcite (white), and (b) sulfhydrylbystrite (orange, Sample 3) in association with afghanite (pale blue), diopside (dark greyish-green to almost black), plagioclase (yellow to beige), and calcite (white). The fields of view are 15 mm across in both photos.

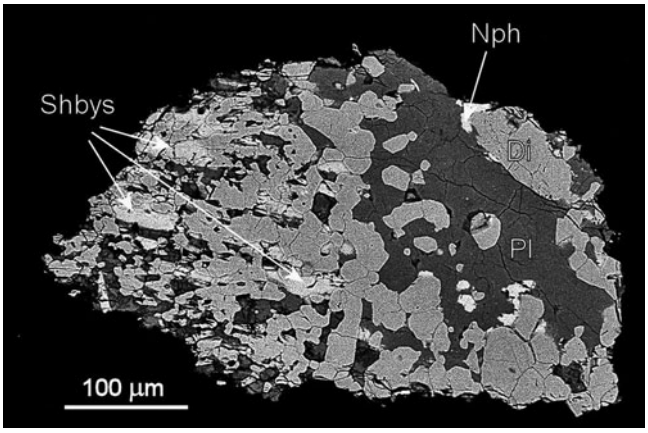

Figure 3. Sulfhydrylbystrite (Shbys) in association with nepheline (Nph), phlogopite (Pl), diopside (Di) and nepheline (Nph). Sample 3. SEM (BSE) image of a polished section; labels from Warr (2021).

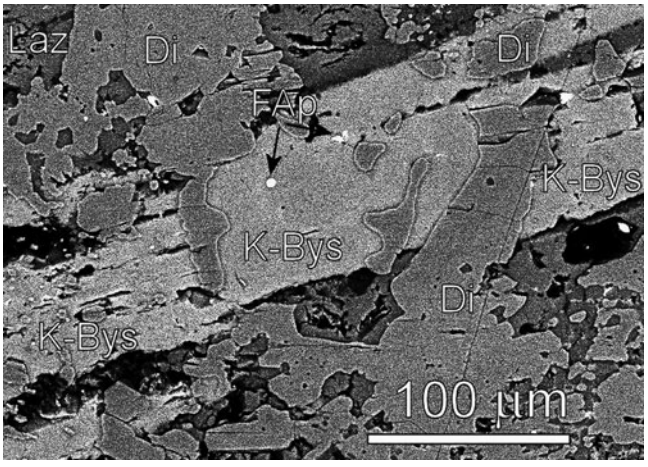

Figure 5. K-rich analogue of bystrite (K-Bys) in association with diopside (Di), lazurite (Laz) and fluorapatite (FAp). Sample 4. SEM (BSE) image of a polished section; labels from Warr (2021).

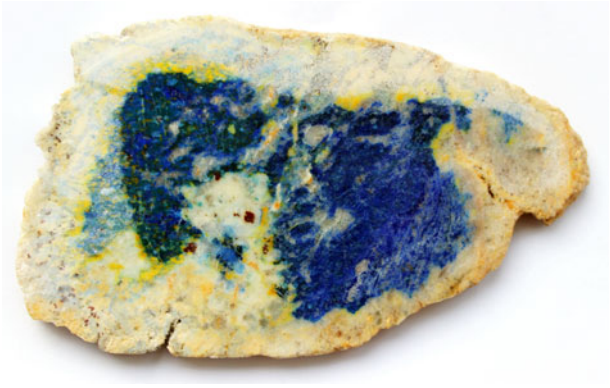

Figure 4. K-rich analogue of bystrite forming microscopic grains in the yellow zone of metasomatite between zones enriched in lazurite (blue) and diopside (light grey, with inclusions of white calcite and blue lazurite). Polished section of Sample 4. The field of view is 14 cm across.

and calcite. The thin outer zone of the boudin is composed of a phlogopite–fluorapatite–calcite aggregate. The working number of Sample 4 in the Vinogradov Institute of Geochemistry, Siberian Branch of Russian Academy of Sciences is 1256.

Experimental methods and data processing

In order to obtain the infrared (IR) absorption spectra, powdered samples were mixed with dried KBr, pelletised, and analysed using an ALPHA FTIR spectrometer (Bruker, 2007) in the range 360–4000 cm^{-1} with a resolution of 4 cm^{-1}. A total of 16 scans were collected for each spectrum. The IR spectrum of an analogous pellet of pure KBr was used as a reference.

Raman spectra of randomly oriented samples were obtained using an EnSpectr R532 spectrometer based on an OLYMPUS CX 41 microscope coupled with a diode laser ($\lambda = 532$ nm) at room temperature. The spectrum was recorded in the range of 100 to 4000 cm^{-1} with a diffraction grating of 1800 gr mm^{-1}

https://doi.org/10.1180/mgm.2023.29 Published online by Cambridge University Press

and a spectral resolution of 6 cm^{-1}. The radiation power at the output of the laser source was ~5 mW. The diameter of the focal spot on the sample was <5 μm. The back-scattered Raman signal was collected with a 40× objective; signal acquisition time for a single scan of the spectral range was 1 s; and the signal was averaged over 50 scans. Crystalline silicon was used as a calibration standard. The shape of the luminescent spectrum profile was corrected according to a standard procedure based on subtracting a profile of the same shape, constructed as a superposition of a set of Lorentz lines with half-widths exceeding a limiting value. The limiting half-width value was 100 cm^{-1}.

Six spot analyses of Sample 1 were obtained in the Vinogradov Institute of Geochemistry, Irkutsk, Russia with a JXA_8200 Jeol electron microscope equipped with a wave dispersion spectrometer operated at an acceleration voltage of 20 kV, a current intensity of 10 nA and a counting time of 10 s. The beam was defocused to 20 μm to decrease the thermal effect on the sample. Under these conditions, the mineral was stable with respect to the beam effect. The following standards and analytical lines were used: pyrope (Si*K*α), albite (Al*K*α and Na*K*α), diopside (Ca*K*α), orthoclase (K*K*α), baryte (S*K*α) and chlorapatite (Cl*K*α).

Five electron microprobe analyses of Sample 2 were carried out in the Korzhinskii IInstitute of Experimental Mineralogy RAS, Chernogolovka, Russia, on an analytical suite including a digital scanning electron microscope (SEM) Tescan VEGA-II XMU (produced by Tescan Orsay Hld., Brno, Czech Republic) equipped with an energy-dispersive spectrometer (EDS) INCA Energy 450 with a wavelength dispersive spectrometer (WDS) Oxford INCA Wave 700, The EDS analyses were performed with an accelerating voltage of 20 kV, current of 65 to 80 pA, beam diameter of 120 nm and a counting time of 100 s. The beam was defocused to 20 μm to decrease the thermal effect on the sample. Under these conditions, the mineral was stable with respect to the beam effect. The following standards were used: CaF_2 for F, albite for Na, synthetic Al_2O_3 for Al, wollastonite for Ca, potassium feldspar for K, SiO_2 for Si, Fe metal for Fe, FeS_2 for S and NaCl for Cl. Contents of other elements with atomic numbers > 6 are below their detection limits. The contents of all components obtained using test WDS analysis of Sample 2 (performed with an accelerating voltage of 20 kV and a current of 1–2 nA) coincide with the data obtained using the EDS-mode analysis within 1–2 rel.%.

Powder X-ray diffraction data (Kaneva *et al.*, 2017; Sapozhnikov *et al.*, 2017) were collected using a D8 ADVANCE Bruker diffractometer equipped with a Göbel mirror and VÅNTEC-1 PSD detector with radial Soller slits on the diffraction beam. Data were recorded in step scan mode in the 2θ range from 5 to 70°, using Cu*K*α radiation. The experimental conditions were as follows: voltage of 40 kV, current of 40 mA, time per step of 1 s, and 2θ step size of 0.02°. *VESTA* (version 4.3.0) software (Momma and Izumi, 2011) was used to simulate the X-ray diffraction pattern of bystrite using the crystal-structure model by Sapozhnikov *et al.* (2017). Unit-cell parameters were refined from the powder data using *TOPAS 4* software (Bruker, 2008).

Results

Physical properties

Bystrite Samples 1 and 2 are yellow with vitreous lustre and pale yellow streak. A weak luminescence is observed under a λ = 532 nm laser beam. Bystrite is brittle, with Mohs hardness of 5 and distinct cleavage: on {10$\bar{1}$0}. The fracture is uneven. Density measured by flotation in heavy liquids (bromoform + heptane) is equal to 2.43(1) g·cm^{-3} for Sample 1 (Sapozhnikov *et al.*, 1991) and to 2.42(1) g·cm^{-3} for Sample 2. Density calculated using the empirical formula and unit-cell volume refined from single-crystal XRD data equals 2.412 g cm^{-3} (for Sample 1) and 2.428 g cm^{-3} (for Sample 2).

In plane-polarised light (λ = 589 nm), bystrite is yellow. The mineral is uniaxial (+). The refractive indices for Sample 1 are: ε = 1.660(2) and ω = 1.584(2). Pleochroism is strong: deep yellow on N_e and colourless on N_o.

Infrared spectroscopy

The IR spectra of bystrite and sulfhydrylbystrite (Fig. 6) are similar. The distinctive features of sulfhydrylbystrite are the bands at 3565, 3460 and 1645 cm^{-1} corresponding to stretching and bending vibrations of H_2O molecules as well as a weak band at 2556 cm^{-1} corresponding to stretching vibrations of the HS^- anion. The incorporation of H_2O molecules in the structure of sulfhydrylbystrite is possible because of a deficit of S_5^{2-} anionic groups (0.86 groups per formula unit in the empirical formula: Sapozhnikov *et al.*, 2017). Weak bands at 3430 and 1628 cm^{-1} in the IR spectrum of bystrite are related to water adsorbed by KBr.

Based on high-level *ab initio* calculations, the wavenumbers of fundamental S–S stretching vibrations predicted for S_5^{2-} coordinated by Li^+ are 471, 463 and 416 cm^{-1} (Steudel and Chivers, 2019). Similar bands are observed in the IR spectra of bystrite and sulfhydrylbystrite in the ranges of 413–422 and 454–466 cm^{-1}. No bands in these ranges are in the IR spectrum of carbobystrite, a carbonate cancrinite-group mineral with the bystrite-type framework (Chukanov, 2014).

Raman spectroscopy

A weak luminescence of bystrite is observed under laser beam, unlike sulfhydrylbystrite that shows a strong luminescence under the same conditions (Fig. 7).

The strongest band of SO_4^{2-} in Raman spectra of sulfate minerals belonging to the cancrinite and sodalite groups is observed in the range of 970–990 cm^{-1} (Chukanov *et al.*, 2020a, 2020b, 2022b; Sapozhnikov *et al.*, 2021). This band is absent in the Raman spectra of bystrite Sample 2 (see chemical data below) and sulfhydrylbystrite Sample 3 (Fig. 8).

In the ranges of S–S stretching (410–540 cm^{-1}) and S–S–S bending (170–240 cm^{-1}) vibrations, both spectra contain a strong doublet and a strong single band, respectively. In the Raman spectra of minerals belonging to the sodalite–sapozhnikovite solid-solution series with the general formula $Na_8(Al_6Si_6O_{24})(Cl,HS)_2$, bands in the ranges of 459–464 and 254–260 cm^{-1} are related to stretching and bending vibrations of the $[(Cl,HS)Na_4]^{3+}$ clusters (Chukanov *et al.*, 2022b). Thus, the peak at 505 cm^{-1} in the Raman spectrum of bystrite and the peak at 508 cm^{-1} in the Raman spectrum of sulfhydrylbystrite are to be assigned to S–S stretching vibrations of the S_5^{2-} anion occurring in the structures of these minerals. The bands at 442 and 447 cm^{-1} may be either resonance modes involving S–S and Na–(Cl,HS) stretching vibrations or a result of overlapping of S–S and Na–(Cl,HS) stretching bands. Correspondingly, the peaks at 187 and 189 cm^{-1} are due to S–S–S bending vibrations of S_5^{2-}, whereas the peaks at 250 and 255 cm^{-1} are due to Na–(Cl,SH) stretching vibrations.

The strong band of H–S stretching vibrations observed in the Raman spectrum of sulfhydrylbystrite at 2562 cm^{-1} is close to the

https://doi.org/10.1180/mgm.2023.29 Published online by Cambridge University Press

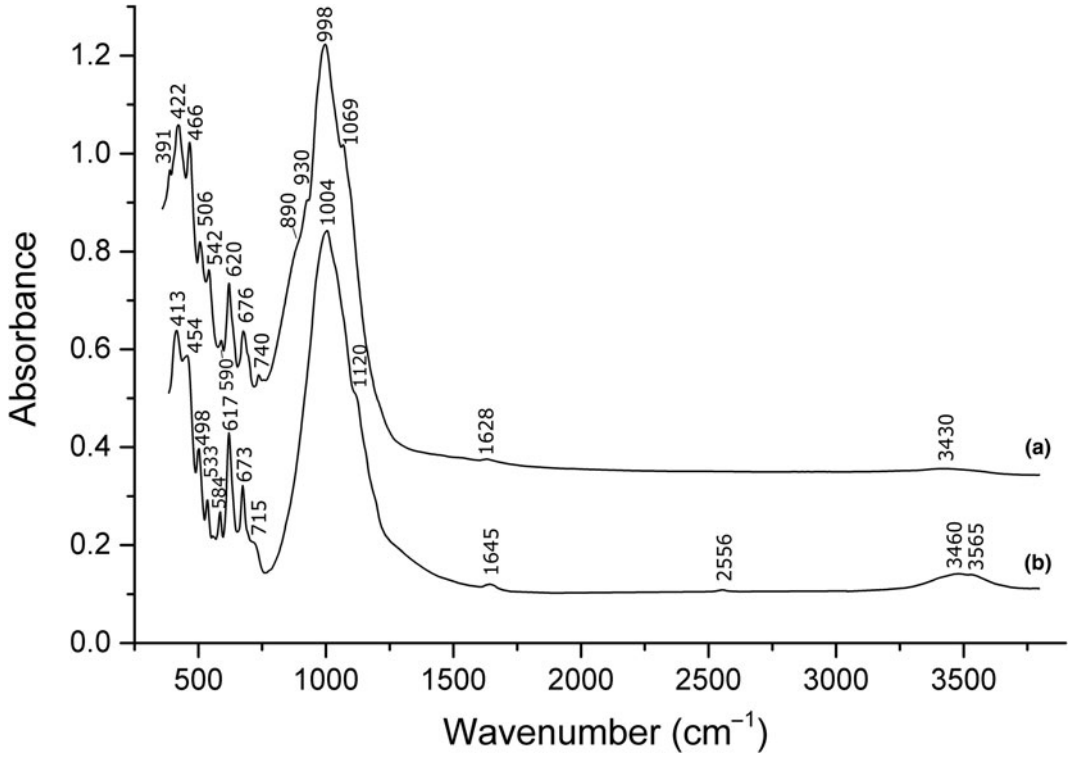

Figure 6. Powder infrared absorption spectra of (a) bystrite (Sample 2) and (b) sulfhydrylbystrite.

band at 2553 cm^{-1} corresponding to the of H–S stretching vibrations of the HS^- anion in sapozhnikovite $Na_8(Al_6Si_6O_{24})(Cl,HS)_2$ (Chukanov *et al.*, 2022b). The analogous band in the Raman spectrum of bystrite Sample 2 (at 2557 cm^{-1}) is much weaker, which is in agreement with the chemical composition of this mineral.

Most probably, the Raman band of bystrite at 845 cm^{-1} is an overtone of the band at 442 cm^{-1}. All other (weak) bands in the Raman spectrum of bystrite correspond to vibrations of the aluminosilicate framework.

A specific feature of the red–orange sulfhydrylbystrite variety distinguishing it from yellow bystrite is a series of additional weak Raman bands at 327, 362, 395 and 667 cm^{-1}. Similar bands (at 330, 373 and 674 cm^{-1}) are predicted for the *cis*-S_4 neutral molecule based on high-level *ab initio* calculations (Eckert and Steudel, 2003). The presence of *cis*-S_4 (planar non-cyclic $C2_v$ isomer), that is a strong red chromophore (Rejmak, 2020; Chukanov *et al.*, 2022) in red–orange sulfhydrylbystrite is in agreement with its colour, different from the yellow colour of bystrite. Note that the acyclic *cis*-S_4 isomer is the most thermodynamically stable (Eckert and Steudel, 2003; Wong and Steudel, 2003; Rejmak, 2020). This molecule was also detected in a number of sodalite-group minerals from the Malo–Bystrinskoe deposit (Chukanov *et al.*, 2020a, 2022a).

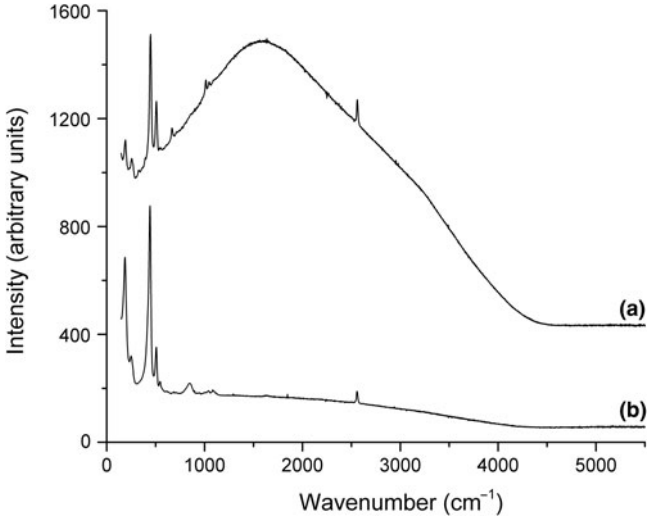

Figure 7. Uncorrected Raman spectra of (*a*) sulfhydrylbystrite, Sample 3 and (*b*) bystrite, Sample 2 showing different intensities of luminescence.

Another specific feature of the sulfhydrylbystrite studied is the weak Raman band at 607 cm^{-1} corresponding to a minor admixture of the $S_2^{\bullet-}$ radical anion that is the cause of strong luminescence of red–orange sulfhydrylbystrite and some sodalite-group minerals, including the recently approved species, sapozhnikovite (Chukanov *et al.*, 2022b) and bolotinaite (Chukanov *et al.*, 2022c). A weak luminescence of bystrite Sample 2 under the laser beam and the absence of a detectable band at ~607 cm^{-1} indicate that the $S_2^{\bullet-}$ radical anion may only occur in this mineral in trace amounts.

The assignment of Raman bands was carried out in accordance with data from Eckert and Steudel (2003), Steudel and Chivers (2019), Rejmak (2020) and Chukanov *et al.* (2020a, 2020b; 2022a, 2022b, 2022d).

Chemical data

Analytical data are given in Table 1. Sample 1 is a S-deficient variety of bystrite. Taking into account that according to the wet chemical analyses 4% of total sulfur may occur in the sulfate form (Sapozhnikov *et al.*, 1991), total sulfur was divided among

https://doi.org/10.1180/mgm.2023.29 Published online by Cambridge University Press

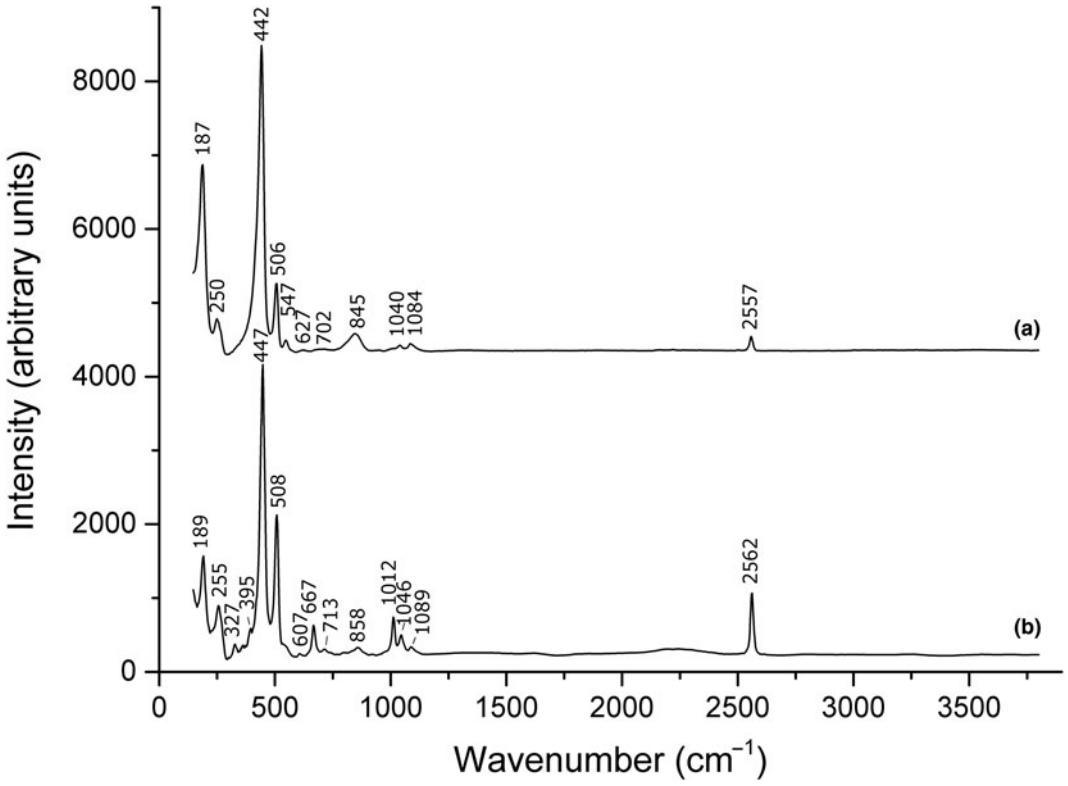

Figure 8. Corrected Raman spectra of (*a*) bystrite, Sample 2 and (*b*) sulfhydrylbystrite, Sample 3.

S_5^{2-} and SO_4^{2-} based on the charge-balance requirement. Sample 2 is more S-rich. According to the Raman spectrum, this sample contains minor HS^- admixture.

The empirical formula of Sample 1 based on $(Si,Al)_{12}$ is $Na_{6.97}K_{0.04}Ca_{0.98}(Si_{6.03}Al_{5.97}O_{24})(S_5^{2-})_{0.93}[(SO_4^{2-})_{0.15}Cl_{0.83}]$.

The empirical formula of Sample 2 based on $(Si,Al)_{12}$ is $Na_{6.75}K_{0.04}Ca_{1.11}(Si_{6.09}Al_{5.91}O_{24})(S_5^{2-})_{1.04}[(HS^-)_{0.17}Cl_{0.85}]$ (sulfur is divided among S_5^{2-} and HS^- taking into account the charge-balance requirement). Some excess of extra-framework anions (2.06 instead of the theoretical value of 2) may be due to a minor admixture of the $S_2^{\bullet-}$ radical anion and/or analytical error.

The idealised end-member formula of bystrite is $Na_7Ca(Al_6Si_6O_{24})S_5^{2-}Cl^-$. It requires (wt.%): Na_2O 19.53, CaO 5.05, Al_2O_3 27.53, SiO_2 32.44, S 14.43, Cl 3.19, $-O{\equiv}S_5^{2-}$ −1.44, $-O{\equiv}Cl^-$ −0.73, total 100.00.

X-ray diffraction and crystal structure

Powder X-ray diffraction data for bystrite are given in Table 2. The unit-cell parameters of Sample 2 refined from the powder data are: $a = 12.852(1)$ Å, $c = 10.692(1)$ Å and $V = 1529.39(1)$ Å^3.

Table 1. Chemical composition (wt.%) of bystrite.

Sample 1 (WDS-mode analyses)*				Sample 2 (EDS-mode analyses)**			
Component	Mean	Ranges	Standard deviation	Component	Mean	Ranges	Standard deviation
Na_2O	19.51	19.06–19.92	0.38	Na_2O	18.70	18.38–19.31	0.28
K_2O	0.16	0.06–0.28	0.08	K_2O	0.16	0.08–0.29	0.08
CaO	4.97	4.53–5.21	0.27	CaO	5.55	4.91–5.95	0.41
Al_2O_3	27.61	26.79–27.84	0.41	Al_2O_3	26.95	26.20–27.43	0.46
Fe_2O_3	0	0	0	Fe_2O_3	0.03	0–0.11	0.05
SiO_2	32.72	31.41–33.49	0.75	SiO_2	32.68	31.88–33.64	0.73
S_5^{2-}	13.46	13.33–14.27	0.32	S_5^{2-}	14.87	14.69–15.50	0.31
SO_3	1.08	(for total sulfur)	(for total sulfur)	HS^-	0.51	(for total sulfur)	(for total sulfur)
Cl^-	2.66	2.56–2.80	0.10	Cl^-	2.70	2.39–2.90	0.19
$-O{\equiv}S_5^{2-}$	−1.34	-	-	$-O{\equiv}S_5^{2-}$	−1.48	-	-
				$-O{\equiv}HS^-$	−0.12	-	-
$-O{\equiv}Cl^-$	−0.60	-	-	$-O{\equiv}Cl^-$	−0.61	-	-
Total	100.23	-	-	Total	99.94	-	-

*Based on the wet chemical analysis, up to 4% of total sulfur in Sample 1 may occur in the sulfate form (Sapozhnikov *et al.*, 1991). Sulfur is divided among S_5^{2-} and SO_4^{2-} taking into account the requirement of charge balance in the empirical formula (see text).

**The Raman spectrum shows the presence of minor HS^- admixture in Sample 2. Bands of SO_4^{2-} are not observed in the Raman spectrum of this sample. Sulfur is divided among S_5^{2-} and HS^- taking into account the requirement of charge-balance in the empirical formula (see text).

https://doi.org/10.1180/mgm.2023.29 Published online by Cambridge University Press

Table 2. Powder X-ray diffraction data of bystrite and sulfhydrylbystrite.

Bystrite						Sulfhydrylbystrite		
Sample 1 (Sapozhnikov *et al.*, 1991)		Sample 2 (Kaneva *et al.*, 2017)				Sapozhnikov *et al.*, 2017		
I_{obs} (%)	d_{obs} (Å)	I_{obs} (%)	d_{obs} (Å)	I_{calc}* (%)	d_{calc}** (Å)	I_{obs} (%)	d_{obs} (Å)	*h k l*
2	11.2	11	11.2	4	11.1	–	–	100
1	7.71	8	7.731	2	7.710	13	7.757	101
7	6.44	9	6.436	8	6.426	15	6.480	110
5	4.944	7	4.944	2	4.937	–	–	201
70	**4.824**	**32**	**4.821**	**18**	**4.819**	48	4.857	102
5	4.212	8	4.210	–	–	10	4.248	210
1	4.112	5	4.114	–	–	9	4.136	112
80	**3.919**	**38**	**3.915**	**10**	**3.915**	38	3.948	211
100	**3.720**	**100**	**3.712**	**100**	**3.710**	94	3.739	300
25	3.396	16	3.394	11	3.394	25	3.417	103
90	**3.313**	**50**	**3.307**	**20**	**3.306**	100	3.331	212
3	3.221	6	3.216	8	3.213	–	–	220
10	2.969	9	2.966	3	2.966	–	–	311
25	**2.784**	**18**	**2.782**	**26**	**2.783**	25	2.805	400
35	**2.694**	**22**	**2.692**	**24**	**2.693**	32	2.715	401
70	**2.676**	**30**	**2.673**	**35**	**2.673**	56	2.692	004
2	2.600	5	2.600	3	2.599	7	2.618	104
35	**2.471**	**23**	**2.468**	**51**	**2.468**	28	2.487	402
2	2.334	5	2.332	4	2.333	8	2.349	313
2	2.304	4	2.303	3	2.304	–	–	322
10	2.194	7	2.193	15	2.193	15	2.211	403
2	2.169	5	2.169	5	2.169	8	2.183	304
20	2.142	15	2.142	–	–	27	2.156	330
10	2.094	8	2.090	–	–	–	–	420
7	2.056	6	2.054	–	–	13	2.070	224
5	2.013	7	2.011	–	–	–	–	413
7	1.928	6	1.927	8	1.928	11	1.941	404
5	1.906	9	1.904	–	–	–	–	215
5	1.872	9	1.869	–	–	7	1.888	512
15	1.799	10	1.798	4	1.798	19	1.881	414
8	1.782	8	1.782	3	1.782	10	1.796	520
3	1.758	4	1.758	–	–	–	–	521
5	1.731	6	1.730	2	1.731	–	–	432
–	–	–	–	–	–	8	1.772	106
3	1.695	5	1.696	5	1.695	6	1.710	405
1	1.671	3	1.673	–	–	6	1.682	334
3	1.641	4	1.640	2	1.641	–	–	325
–	–	–	–	–	–	10	1.653	216
5	1.606	6	1.606	10	1.607	12	1.615	514
–	–	–	–	–	–	6	1.584	531
2	1.571	4	1.572	–	–	–	–	701
–	–	–	–	–	–	10	1.536	532
–	–	7	1.523	2	1.524	–	–	604
–	–	5	1.501	9	1.501	10	1.523	434
–	–	–	–	–	–	9	1.510	425
–	–	–	–	–	–	11	1.486	710
–	–	–	–	–	–	7	1.460	533
1	1.438	4	1.436	–	–	–	–	416
10	1.377	8	1.377	7	1.377	13	1.388	444

*For the calculated pattern, only reflections with intensities ≥1 are given.
**For the unit-cell parameters calculated from single-crystal data.
The strongest reflections are marked in bold type.

The crystal structure of bystrite was first solved on Sample 1 (Pobedimskaya *et al.*, 1991) and then refined on Sample 2 (Sapozhnikov *et al.*, 2017; Kaneva *et al.*, 2017). The structure is based on a Losod-type aluminosilicate framework with the *ABAC* stacking sequence.

Based on the <*T*–O> distances in the Si- and Al-centred tetrahedra (<Si1–O> = 1.614(3) Å, <Si2–O> = 1.615(3) Å, <Al1–O> = 1.731(4) Å and <Al2–O> = 1.729(4) Å; Sapozhnikov *et al.*, 2017) it is concluded that Si and Al are fully ordered in the crystal structure. The Si–Al framework contains two kinds of cages, small cancrinite (CAN) and larger Losod (LOS) ones. The crystal structure of bystrite is illustrated in Figs 9 and 10.

Two extra-framework cation sites (*M*1 and *M*2, Fig. 9a) are situated at the centres of the bases of the cages and are occupied by Ca and Na, respectively. The *M*3 and *M*4 positions within the LOS cages (Fig. 9a) are split into pairs of sub-sites which are partly occupied by Na (Fig. 10). The *X*6 site (Fig. 9a) located inside the cancrinite cage on the three-fold axis is occupied by

https://doi.org/10.1180/mgm.2023.29 Published online by Cambridge University Press

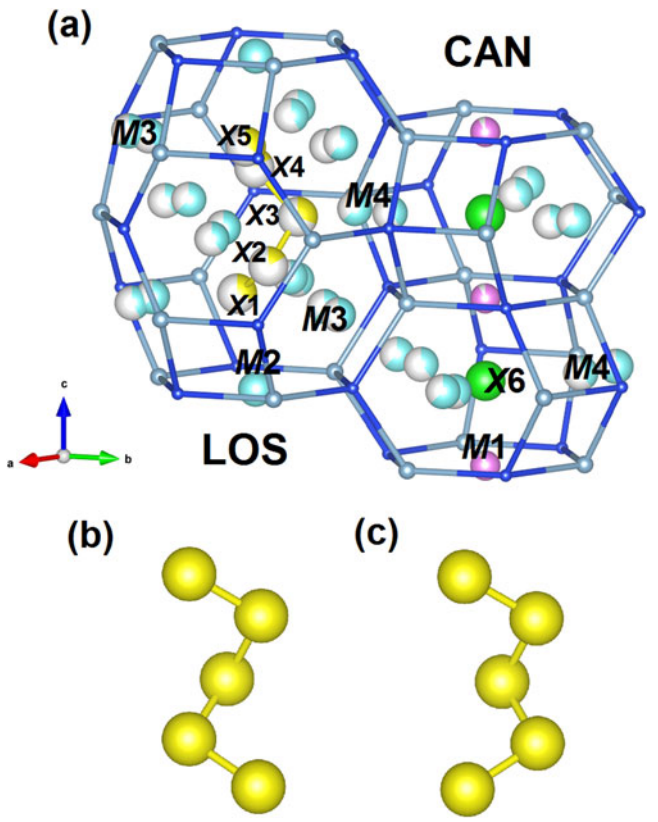

Figure 9. A fragment of the bystrite crystal structure showing (a) the contents of the Losod (LOS) and two cancrinite (CAN) cages as well as *trans*- (b) and *cis*- (c) conformers of the S_5^{2-} polysulfide ion. Small blue and pale blue spheres are Si and Al atoms, respectively. The partially white colouring of some spheres indicates the fraction of vacancies at corresponding sites.

Cl^-. The LOS cage contains the S_5^{2-} anion which is stretched along [001]. The S_5^{2-} anion has a chain configuration. The sulfur atoms are disordered in such a way that *trans*- or *cis*-conformers of S_5^{2-} alternate in the structure (Fig. 9b,c). The S atoms belonging to S_5^{2-} occupy the *X*1–*X*5 sites and coordinate the *M*2–*M*4 sites (Fig. 9a). A small amount of Ca^{2+} may occur at the *M*2 site, as suggested by excess of Na^+ occupancy (~1.1) and chemical data.

Isomorphism of cancrinite-group minerals with the bystrite-type framework

Chemical variations of S-bearing bystrite-type are mainly determined by the substitutions of Na^+ *vs.* K^+ at the *M*4 site and HS^- *vs.* Cl^- at the *X*6 site. All minerals belonging to the bystrite–sulfhydrylbystrite solid solution described previously are close to the bystrite or sulfhydrylbystrite end-members [$Na_7Ca(Al_6Si_6O_{24})S_5^{2-}Cl^-$ and $Na_5K_2Ca(Al_6Si_6O_{24})S_5^{2-}(HS)^-$, respectively].

Sample 4 is an exception to this regularity. Its chemical composition is given in Table 3. The empirical formula of Sample 4 is $Na_{4.64}K_{1.65}Ca_{1.40}(Si_{6.17}Al_{5.81}Fe_{0.02}O_{24})S_{4.98}Cl_{0.72}$ where S is total sulfur. By analogy with other bystrite-type minerals, one can suppose that a major part of sulfur in Sample 4 belongs to the S_5^{2-} anion. Sample 4 is characterised by rather wide variations of the contents of extra-framework cations (Na, K and Ca) whereas the contents of S and Cl are more stable.

Unfortunately, no other data could be obtained for Sample 4 because of very small sizes of its individual crystals and their intimate intergrowths with associated minerals.

Carbobystrite, $Na_8(Al_6Si_6O_{24})(CO_3)\cdot 4H_2O$ (Khomyakov *et al.*, 2010) crystallised in a late state of peralkaline pegmatite formation, at a high activity of CO_2 and H_2O. Among associated minerals, there are hydrous silicates (natrolite, umbite and members of the labuntsovite group). Sulfur is concentrated in

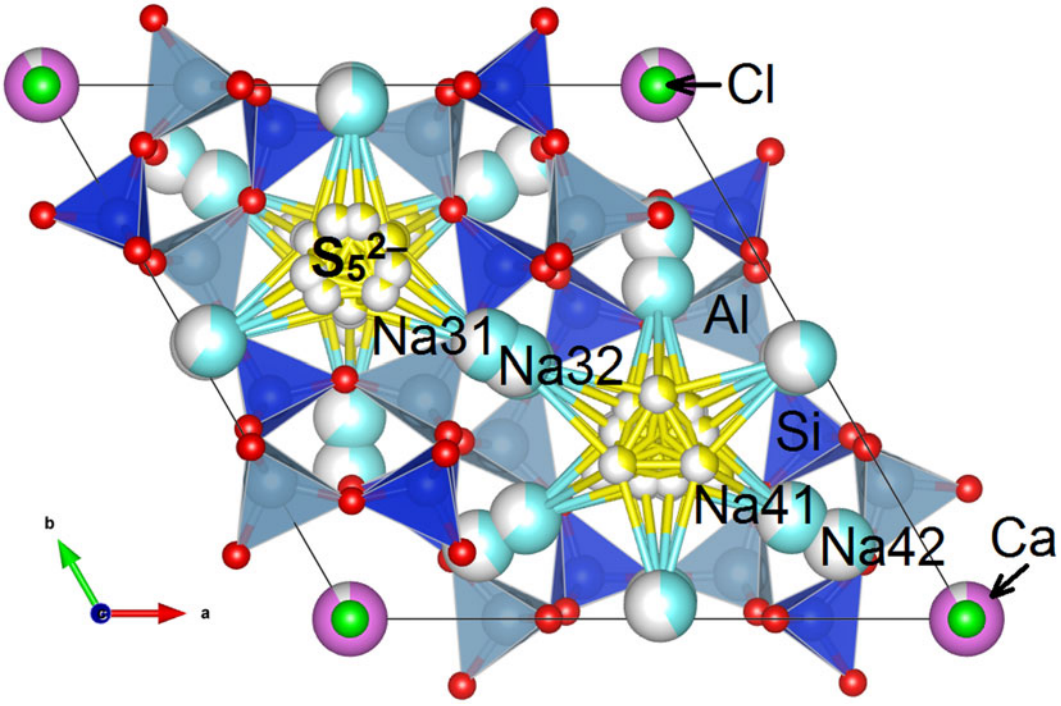

Figure 10. The crystal structure of bystrite projected along the *c* axis. Si and Al tetrahedra are blue and pale blue, respectively; Ca and Na atoms are purple and cyan, respectively. Oxygen atoms are drawn in red, Cl atoms are drawn in green. The positions of S atoms are yellow. The unit cell is outlined.

https://doi.org/10.1180/mgm.2023.29 Published online by Cambridge University Press

Table 3. Chemical composition (wt.%) of Sample 4.*

Component	Mean	Range	Standard deviation
Na_2O	12.69	11.00–14.29	1.30
K_2O	6.85	4.94–7.84	1.05
CaO	6.90	5.96–8.37	1.00
Al_2O_3	26.16	25.87–26.39	0.19
Fe_2O_3	0.09	0–0.16	0.07
SiO_2	32.74	31.32–33.46	0.78
S_5^{2-}	14.11	13.70–14.45	0.29
Cl^-	2.24	1.93–2.46	0.19
$-O\equiv S_5^{2-}$	−1.41	-	-
$-O\equiv Cl^-$	−0.51	-	-
Total	99.86	-	-

*Note: All sulfur is given as S_5^{2-}.

associated sulfides of chalcophile elements (sphalerite and galena). As a result, carbobystrite does not contain Ca and S. There is no evidence of solid solution among carbobystrite and bystrite–sulfhydrylbystrite.

Comparative data for bystrite, sulfhydrylbystrite and carbobystrite are given in Table 4.

Discussion

Raman spectroscopy is a sensitive tool used to detect polysulfide species (Eckert and Steudel, 2003; Chukanov *et al.*, 2020a, 2020b; Sapozhnikov *et al.*, 2021; Chukanov *et al.*, 2022a, 2022b, 2022c, 2022d). Both bystrite and sulfhydrylbystrite show strong Raman bands corresponding to the S_5^{2-} anion which is a yellow chromophore. These minerals are the only mineral species containing S_5^{2-} as a species-defining component. The lack of isomorphism in the bystrite/carbobystrite relationship may be due to the lack of available samples. Possibly, chemical differences between these minerals are due to geochemical rather than crystal-chemical factors. At least, in minerals belonging to the sodalite–sapozhnikovite solid-solution series a wide isomorphism involving Cl^- and HS^- is observed (Chukanov *et al.*, 2022b).

In bystrite, the HS^- anion is absent or occurs in minor amounts. However, its presence in sulfhydrylbystrite and some bystrite varieties is important because it is an indicator of highly reducing conditions. This matter was discussed in reference to the formation of the HS^--dominant sodalite-group mineral sapozhnikovite, $Na_8(Al_6Si_6O_{12})(HS)_2$, and associated oxalate-dominant cancrinite-group mineral kyanoxalite, $Na_7(Al_{5-6}Si_{6-7}O_{24})(C_2O_4)_{0.5-1.0}\cdot 5H_2O$, under reducing conditions which appeared as a result of aegirine crystallisation (Chukanov *et al.*, 2022b).

It was also shown (Chukanov *et al.*, 2022a) that the conversion of SO_4^{2-} and $S_3^{\bullet-}$ into HS^- coupled with the conversion of CO_2 into $C_2O_4^{2-}$ takes place in slyudyankaite and other sodalite-group minerals from the Malo–Bystrinskoe deposit after their heating under reducing conditions (over the Fe–FeS buffer) at 700°C. The by-products of these transformations are S_4, $S_4^{\bullet-}$ and $S_2^{\bullet-}$.

Sapozhnikovite, sulfhydrylbystrite and bystrite are the only minerals in which the presence of HS^- was reliably detected. These minerals are the only feldspathoids containing all or almost all sulfur in the sulfide form.

Unlike most sodalite-group minerals from the Malo–Bystrinskoe deposit, sapozhnikovite contains only trace amounts of CO_2 molecules which were partly converted to COS molecules (Chukanov *et al.*, 2022b). Similarly, sulfhydrylbystrite and bystrite do not contain CO_2 molecules in amounts detectable by routine IR spectroscopy.

Marbles that are among the host rocks of lazurite-bearing bodies are locally enriched in graphite and pyrite (Ivanov and Sapozhnikov, 1985), which could be a cause of reducing conditions in the formation of bystrite.

As noted above, most available analyses of bystrite and sulfhydrylbystrite correspond to samples close to the end-members of these minerals, i.e. K-rich samples are Cl-depleted and Cl-rich samples are K-depleted. Most likely, this regularity has a geochemical rather than crystal-chemical cause because there are no significant differences between crystal-chemical characteristics (charges, effective radii and force constants) of Cl^- and HS^-. The existence of a K- and Cl-rich bystrite-type mineral with the

Table 4. Comparative data for bystrite, sulfhydrylbystrite and carbobystrite.

Mineral	Bystrite	Sulfhydrylbystrite	Carbobystrite
Simplified formula	$Na_7Ca(Al_6Si_6O_{24})S_5^{2-}Cl^-$	$Na_5K_2Ca(Al_6Si_6O_{24})S_5^{2-}(HS)^-$	$Na_8(Al_6Si_6O_{24})(CO_3)\cdot 4H_2O$
Symmetry	Trigonal	Trigonal	Trigonal
Space group	*P*31*c*	*P*31*c*	*P*31*c*
a (Å)	12.8527	12.9567	12.6678
c (Å)	10.6907	10.7711	10.3401
Z	2	2	2
Strong lines of the powder X-ray diffraction pattern: *d*, Å (*I*, %)	4.821 (32) 3.915 (38) 3.712 (100) 3.307 (50) 2.782 (18) 2.692 (22) 2.673 (30) 2.468 (23)	4.857 (48) 3.948 (38) 3.739 (94) 3.331 (100) 2.715 (32) 2.692 (56) 2.487 (28) 2.156 (27)	6.378 (80) 4.689 (100) 3.867 (70) 3.664 (70) 3.249 (100) 2.661 (80)
Optical data	Uniaxial (+) ε = 1.660 ω = 1.584	Uniaxial (+) ε = 1.661 ω = 1.584	Uniaxial (–) ε = 1.488 ω = 1.500
Density (g/cm^3)	2.412 (calculated) 2.42 (measured)	2.368 (calculated) 2.391 (measured)	2.366 (calculated)
Colour	Yellow	Orange	Colourless
References	Sapozhnikov *et al.* (1991); Kaneva *et al.* (2017); this work	Sapozhnikov *et al.* (2017)	Khomyakov *et al.* (2010)

https://doi.org/10.1180/mgm.2023.29 Published online by Cambridge University Press

idealised formula $Na_5K_2Ca(Al_6Si_6O_{24})S_5^{2-}Cl^-$ and species-defining K, S_5^{2-} and Cl^- (Sample 4) confirms this assumption. Moreover, there is a complete solid-solution series between sapozhnikovite and its Cl^- analogue sodalite.

Acknowledgements. The authors are grateful to Owen Missen, Fernando Cámara, Stefan Farsang and an anonymous reviewer for the useful discussion. The crystal-chemical analysis, Raman spectroscopic studies and crystal chemical analysis of bystrite and sulfhydrylbystrite by NVC and MVF were supported by the Russian Science Foundation, grant No. 22-17-00006. Data on infrared spectra and chemical data of associated minerals were obtained in accordance with the state task, state registration number AAAA-A19-119092390076-7.

Competing interests. The authors declare none.

References

Ballirano P., Maras A. and Buseck P.R. (1996) Crystal chemistry and IR spectroscopy of Cl- and SO_4-bearing cancrinite-like minerals. *American Mineralogist*, **81**, 1003–1012, https://doi.org/10.2138/am-1996-7-822

Bruker (2007) *SAINT, version 6.0*. Bruker AXS Inc., Madison, WI, USA.

Bruker (2008) *TOPAS 4*. Bruker AXS Inc., Madison, WI, USA.

Chukanov N.V. (2014) *Infrared Spectra of Mineral Species: Extended Library*. Springer-Verlag GmbH, Dordrecht–Heidelberg–New York–London, 1716 pp.

Chukanov N.V., Sapozhnikov A.N., Shendrik R.Yu., Vigasina M.F. and Steudel R. (2020a) Spectroscopic and crystal-chemical features of sodalite-group minerals from gem lazurite deposits. *Minerals*, **10**, 1042, https://doi.org/10.3390/min10111042.

Chukanov N.V., Vigasina M.F., Zubkova N.V., Pekov I.V., Schäfer C., Kasatkin A.V. and Yapaskurt V.O. (2020b) New aspects of the application of infrared and Raman spectroscopy to the characterization of extra-framework components in sodalite-group minerals. *Minerals*, **10**, 363, https://doi.org/10.3390/min10040363.

Chukanov N.V., Aksenov S.M. and Rastsvetaeva R.K. (2021) Structural chemistry, IR spectroscopy, properties, and genesis of natural and synthetic microporous cancrinite- and sodalite-related materials: a review. *Microporous and Mesoporous Materials*, **323**, 111098, https://doi.org/10.1016/j.micromeso.2021.111098

Chukanov N.V., Shendrik R.Yu., Vigasina M.F., Pekov I.V., Sapozhnikov A.N., Shcherbakov V.D. and Varlamov D.A. (2022a) Crystal chemistry, isomorphism, and thermal conversions of extra-framework components in sodalite-group minerals. *Minerals*, **12**, 887, https://doi.org/10.3390/min12070887

Chukanov N.V., Zubkova N.V., Pekov I.V., Shendrik R.Yu., Varlamov D.A., Vigasina M.F., Belakovskiy D.I., Britvin S.N., Yapaskurt V.O. and Pushcharovsky D.Yu. (2022b) Sapozhnikovite, $Na_8(Al_6Si_6O_{24})(HS)_2$, a new sodalite-group mineral from the Lovozero alkaline massif, Kola Peninsula. *Mineralogical Magazine*, **86**, 49–59, https://doi.org/10.1180/mgm.2021.94

Chukanov N.V., Zubkova N.V., Schäfer C., Pekov I.V., Shendrik R.Yu., Vigasina M.F., Belakovskiy D.I., Britvin S.N., Yapaskurt V.O. and Pushcharovsky D.Yu. (2022c) Bolotinaite, $(Na_6K\square)(Al_6Si_6O_{24})F{\cdot}4H_2O$, a new sodalite-group mineral from the Eifel paleovolcanic region, Germany. *Mineralogical Magazine*, **86**, 920–928, https://doi.org/10.1180/mgm.2022.95.

Chukanov N.V., Shchipalkina N.V., Shendrik R.Yu., Vigasina M.F., Tauson V.L., Lipko S.V., Varlamov D.A., Shcherbakov V.D., Sapozhnikov A.N., Kasatkin A.V., Zubkova N.V. and Pekov I.V. (2022d) Isomorphism and mutual transformations of S-bearing components in feldspathoids with microporous structures. *Minerals*, **12**, 1456, https://doi.org/10.3390/min12111456.

Eckert B. and Steudel F. (2003) Molecular spectra of sulfur molecules and solid sulfur allotropes. *Topics of Current Chemistry*, **231**, 31–97, https://doi.org/10.1007/b13181.

Ivanov V.G. and Sapozhnikov A.N. (1985) *Lazurites of the USSR*. Nauka, Novosibirsk, 172 pp. [in Russian].

Kaneva E.V., Sapozhnikov A.N. and Suvorova L.F. (2017) Crystal structure of chlorinated mineral of cancrinite group with bystrite-type framework. *Crystallography Reports*, **62**, 558–565, https://doi.org/10.1134/S1063774517040071

Khomyakov A.P., Cámara F. and Sokolova E. (2010) Carbobystrite, $Na_8[Al_6Si_6O_{24}](CO_3){\cdot}4H_2O$, a new cancrinite-group mineral species from the Khibina alkaline massif, Kola Peninsula, Russia: Description and crystal structure. *The Canadian Mineralogist*, **48**, 291–300

McCusker L.B., Liebau F. and Engelhardt G. (2001) Nomenclature of structural and compositional characteristics of ordered microporous and mesoporous materials with inorganic hosts. *Pure and Applied Chemistry*, **73**, 381–394, https://doi.org/10.1016/S1387-1811(02)00545-0

Miyawaki R., Hatert F., Pasero M. and Mills S. (2023) Newsletter 70. *Mineralogical Magazine*, **87**, 160–168, doi:10.1180/mgm.2022.135

Momma K. and Izumi F. (2011) VESTA 3 for three-dimensional visualization of crystal, volumetric and morphology data. *Journal of Applied Crystallography*, **44**, 1272–1276, https://doi.org/10.1107/S0021889811038970

Pobedimskaya E.A., Terentieva L.E., Sapozhnikov A.N., Kashaev A.A. and Dorokhova G.I. (1991) Crystal structure of bystrite. *Doklady Akademii Nauk SSSR*, **319**, 873–878 [in Russian].

Rejmak P. (2020) Computational refinement of the puzzling red tetrasulfur chromophore in ultramarine pigments. *Physical Chemistry, Chemical Physics*, **22**, 22684–22698, https://doi.org/10.1039/D0CP03019H.

Rinaldi R. and Wenk H.R. (1979) Stacking variations in cancrinite minerals. *Acta Crystallographica*, **A35**, 825–828, https://doi.org/10.1107/S0567739479001868

Sapozhnikov A.N., Ivanov V.G., Piskunova L.F., Kashaev A.A., Terentieva E.A. and Pobedimskaya L.E. (1991) Bystrite $Ca(Na,K)_7(Si_6Al_6O_{24})(S_3)_{1.5}{\cdot}2H_2O$ – a new cancrinite-like mineral. *Zapiski Vsesyuznogo Mineralogicheskogo Obshchestva* (*Proceedings of the Mineralogical Society of the USSR*), **120**, 97–100 [in Russian].

Sapozhnikov A.N., Kaneva E.V., Suvorova L.F., Levitsky V.I. and Ivanova L.A. (2017) Sulfhydrylbystrite, $Na_5K_2Ca(Al_6Si_6O_{24})(S_5)(SH)$, a new mineral with the LOS framework, and re-interpretation of bystrite: cancrinite-group minerals with novel extra-framework anions, *Mineralogical Magazine*, **81**, 383–402, https://doi.org/10.1180/minmag.2016.080.106

Sapozhnikov A.N., Tauson V.L., Lipko S.V., Shendrik R.Yu., Levitskii V.I., Suvorova L.F., Chukanov N.V. and Vigasina M.F. (2021) On the crystal chemistry of sulfur-rich lazurite, ideally $Na_7Ca(Al_6Si_6O_{24})(SO_4)(S_3)^-{\cdot}nH_2O$. *American Mineralogist*, **106**, 226–234, https://doi.org/10.2138/am-2020-7317.

Steudel R. and Chivers T. (2019) The role of polysulfide dianions and radical anions in the chemical, physical and biological sciences, including sulfur-based batteries. *Chemical Society Reviews*, **48**, 3279–3319 and 4338.

Warr L.N. (2021) IMA-CNMNC approved mineral symbols. *Mineralogical Magazine*, **85**, 291–320, https://doi.org/10.1180/mgm.2021.43

Wong M.W. and Steudel R. (2003) Structure and spectra of tetrasulfur S_4 – an *ab initio* MO Study. *Chemical Physics Letters*, **379**, 162–169, https://doi.org/10.1016/j.cplett.2003.08.026